

# ATLAS BASED AUTOMATED SEGMENTATION OF THE QUADRATUS LUMBORUM MUSCLE USING NON-RIGID REGISTRATION ON MAGNETIC RESONANCE IMAGES OF THE THORACOLUMBAR REGION

V. Jurcak<sup>1</sup>, J. Fripp<sup>1,2</sup>, C. Engstrom<sup>1</sup>, D. Walker<sup>3</sup>, O. Salvado<sup>2</sup>, S. Ourselin<sup>2</sup>, S. Crozier<sup>1</sup>

1. School of ITEE, University of Queensland, Australia, 2. BioMedIA Lab, e-Health Research Center, Australia, 3. Southernex Radiology, Wesley Hospital

## ABSTRACT

Large volume asymmetries of the quadratus lumborum (QL) muscle, determined from time- and expertise-intensive *manual* segmentation of axial magnetic resonance (MR) images, have been associated with an increased risk of developing pars interarticularis stress lesions in the lumbar spine of cricket fast bowlers. The purpose of the present study was to develop an atlas-based *automated* segmentation procedure to determine QL volume from MR images. An MR database of axial lumbar spine images from 15 fast bowlers and 6 athletic control subjects was used to generate the atlas-based segmentation procedures. Initially, all images were preprocessed with a bias field correction algorithm and reverse diffusion interpolation algorithm followed by affine and non-rigid registration methods to generate firstly an average shape atlas (AVG), then based on propagation of manually segmented QL data, develop a probability atlas for automated QL segmentation to calculate muscle volume. The Dice similarity metric (DSC) was used to compare between the QL volume data from the manual and automated segmentation procedures. The mean DICE similarity coefficients between the manual and atlas-based automated segmentation values for the right and left QL muscle volumes were 0.75 (sd=0.1) and 0.76 (sd=0.09), respectively. These preliminary results for the automated segmentation of the QL are encouraging. Further development of the atlas-based segmentation procedures will involve incorporating hierarchical probability atlases for adjacent thoracolumbar muscles to improve the robustness and accuracy of the morphometric analyses obtained by this statistical shape modeling approach.

**Index Terms** - quadratus lumborum, thoracolumbar musculature, automatic segmentation, atlas creation, MRI

## 1. INTRODUCTION

Morphometric analyses of the human thoracolumbar musculature derived from MR images to obtain measures of muscle cross-sectional areas or volumes have been used for examining muscle hypertrophy or atrophy in relation to changing loading milieu [1] and investigating the association between the relative *in vivo* mass of selected paraspinal muscles and lower back pain or injury [2]. In studies published to date, time- and expertise-intensive manual segmentation of the MR images has been used for the morphometric analyses of the thoracolumbar muscles.

The overarching aim of the present research is to develop automated segmentation procedures for fast and robust extraction of accurate and objective morphometric data (e.g., cross-sectional areas, volumes) for the numerous, architecturally complex thoracolumbar muscles. In this paper, we present the procedures for an atlas-based automated segmentation of the quadratus lumborum (QL) volume. Our method involved the generation of an average population atlas from axial MR images of the lumbar region involving affine [3] and non-rigid [4] registration of each case to allow segmentation of the QL using propagation of a probabilistic atlas derived from our existing MR dataset. These segmentations were performed in a leave one out experiment (in terms of atlas creation) and validated against expert manual segmentations using the Dice similarity metric [5].

## 2. MATERIALS AND METHODS

Two MR databases were used in this study. Database A consisted of 21 subjects, including 15 male cricket fast bowlers and 6 athletic control subjects, all aged between 18 and 35 years old. This MR dataset consisted of contiguous 7mm axial images (SE, TR=650ms, TE=15ms, FOV=250mm, 256x256 matrix, in plane resolution 0.98x0.98mm, 2 NEX, Siemens 1.5T Magnetom Vision).

Database B consisted of 3 subjects (contiguous 3mm axial images, SE, TR=590ms, TE=11ms, FOV=400mm, 512x512 matrix, in plane resolution 0.78x0.78mm, 2 NEX, Siemens 1.5T Sonata system). For preliminary analysis of the reproducibility of the atlas-based automated segmentation procedures one subject was examined twice on two different occasions.

Axial images from the entire lumbar region were acquired with a phased-array spinal coil as participants lay supine in the magnet bore with their lower limbs relaxed in extension against the patient table. The medical research ethics committee of the University of Queensland approved all aspects of this research.

### 2.1 Image Processing

All scans were preprocessed with a *bias field correction* algorithm [6]. Database A was also preprocessed with an interpolation algorithm [6]. Figures 1, 2 and 3 illustrate the iterative steps involved in constructing the average shape atlas, generation of the probability atlas for the QL and subsequent validation of the atlas with a leave-one-out method.

### 2.1.1. Inhomogeneity Correction

As a first step for the automated atlas-based segmentation of the QL, a bias-field correction algorithm based on local entropy minimization with a bicubic spline model (LEMS) [6] was used to correct strong intensity inhomogeneities in the MR images. Specifically, it was used for the very steep signal drop-off in the images in dataset A as illustrated in Figure 4.

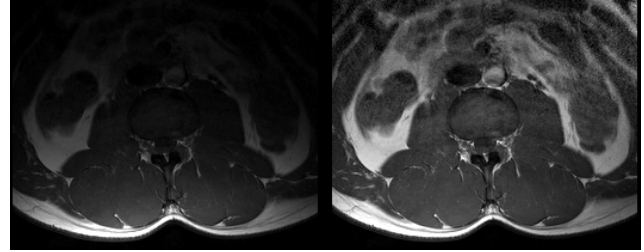


Figure 4. Original image on the left and image corrected with LEMS inhomogeneity correction algorithm on the right.

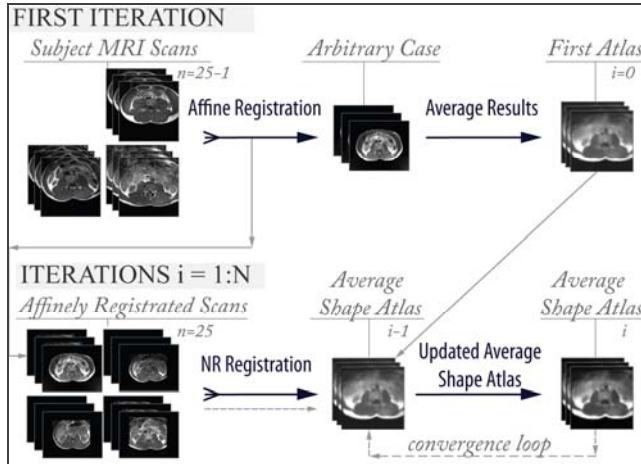


Figure 1. Flow diagram illustrating the process of the Average Shape Atlas creation. The multiple slices represent volume of dataset.

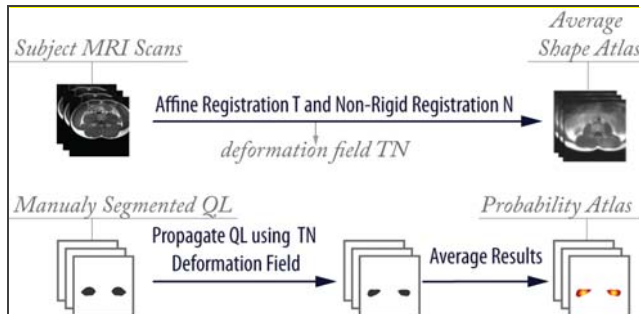


Figure 2. Flow diagram illustrating propagation of manually segmented QL to the atlas space.

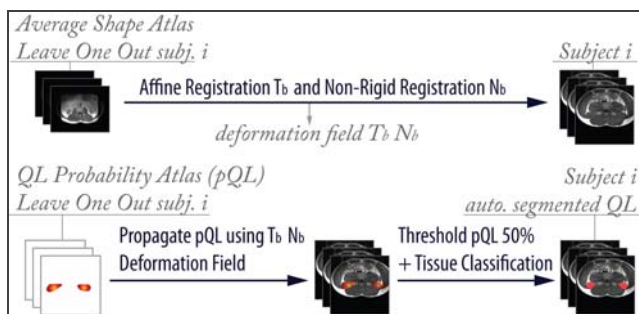


Figure 3. Flow diagram illustrating automatic propagation of QL probabilistic map to segmentation process.

### 2.1.2. Interpolation of Axial Images

To approximate the between-plane resolution of dataset A with dataset B a reverse diffusion interpolation (RDI) algorithm [7] was applied to the original 7mm cross-sectional images of dataset A resulting in an adjusted 0.98x0.98x3.5mm resolution.

Reduction of the section dimensions helps in segmenting elongated anatomical structures like the QL by reducing the anisotropy of the data. This allowed a better match between the atlas and each case as well as improving the visualization of muscle volume and multiplanar reformatted views.

### 2.1.3. Affine Registration

The global transformation between each case and the atlas was estimated by an affine transformation determined from correspondences between very similar areas in both images using a block matching strategy. This procedure has been extensively described in [3] for rigid registration of anatomical sections.

### 2.1.4. Non-Rigid Registration

After affine registration of each case to the average shape atlas (AVG), non-rigid deformation, modeled by a Free Form Deformation (FFD) based on B-splines [4], was used to account for local differences between the case and the average atlas. We used a grid of control points defining a B-splines to determine the deformation. Each grid point was optimized individually to define local deformations. The B-splines were locally controlled, which makes them computationally efficient even for a large number of control points. In this work, a multi-resolution approach of 2 hierarchical levels was used and within each level the spacing between control points was decreased (from 20 to 10 mm).

### 2.1.5. Tissue Classification

Following propagation of the probability atlas for segmentation of the QL, a kmeans tissue classifier was used to exclude any falsely included abdominal fat from the segmented muscle profile. The MR images were assumed to contain four “tissue” classes (background, abdominal fat, muscles, and abdominal viscera) and the intensity was classified using a standard kmeans tissue classification algorithm [ITK].

## 2.2 Atlas Creation and Propagation

In our study we generated an AVG described by Rohlfing [8] (Figure 1). An arbitrary but “representative” case in our database was selected as the initial *reference* case. In the first iteration we registered each of the remaining images to the selected *reference* case using an affine transformation. All the affinely registered cases and the *reference* case were then combined into an average (mean) atlas. Subsequent iterations involved all subjects including

the *reference* case being registered to the average image by non-rigid transformation. After each iteration a new average image was generated and used as the input atlas for the subsequent iteration. A total of 3 iterations were used in this study.

The probabilistic atlas (PA) for the QL was generated (Figure 2) by propagating the manual segmentations of this muscle for each case using the obtained affine and deformation field computed from the MR into the atlas space. The resulting sets of segmentations were then combined into a probabilistic atlas.

### 2.3 Segmentation Process

The bias field corrected and interpolated MR images (LEMS, RDI) were intensity normalized (zero mean and unit variance). These images were then classified using a kmeans algorithm [ITK]. Using a leave one out technique, AVG and probabilistic QL atlases were generated. AVG atlases were registered to the leave out cases and the resulting registrations used to propagate probabilistic QL to the subject MR spaces. Propagated QL atlases were thresholded to 50% and regions classified by k-means as fat were removed (Figure 3).

### 2.4 Validation

The segmentations were performed in a leave one out experiment (in terms of atlas creation) and validated against manual segmentations using the Dice similarity metric ( $DSC = 2(A \cap B) / (A + B)$ ) [5].

## 3.0 RESULTS AND DISCUSSION

### 3.1 Validation of Automatic Segmentation

The complex shape variation seen in the QL is shown in Figure 5. Figure 6 shows average PA and PA overlaid with a probabilistic map of segmented QL. The graph in Figure 7 shows the results of segmentation accuracy - PA with threshold set to 50% improved by tissue classification. The mean DSC coefficient for right and left QL was 0.75 (median = 0.79, std. = 0.1) and 0.76 (median = 0.78, std. = 0.09), respectively.

To illustrate the difference in quality between the automatic and the manual segmentation of the QL volume one case with a high DSC value is compared with two cases with lower DSC values (see Figure 8). The upper pair of images shows the subject with the high DSC value (0.84 for right and 0.86 for left QL). The middle pair of images shows the results for a subject with left-right QL asymmetry of 20% and the lower image displays a subject with distinct bulging of the left QL.

The main causes of segmentation errors are the QL shape variation, the difficulties in detection of muscle contours between QL and surrounding musculature (erector spinae, psoas major and internal abdominal obliques) as well segmentation difficulties in the region where QL is attached to the iliac crest (pelvic bone).

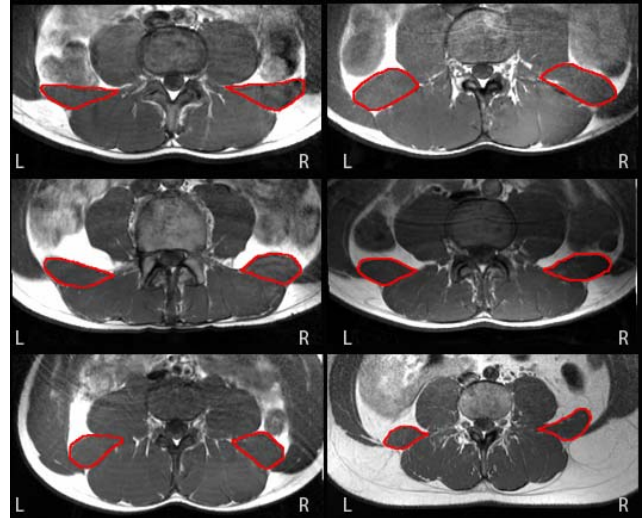


Figure. 5. Manually segmented quadratus lumborum (red contour) at same axial level in 6 representative cases show muscle shape variation, asymmetry and surrounding musculature.

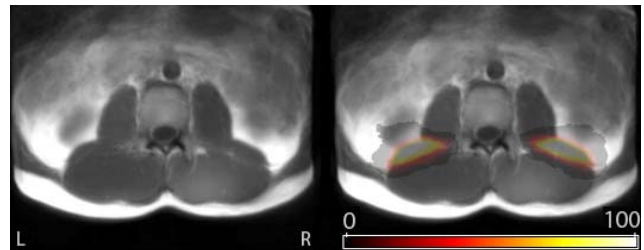


Figure. 6. Axial view of the Average Shape Atlas (left) and same Atlas overlaid with probabilistic map of segmented quadratus lumborum (right).

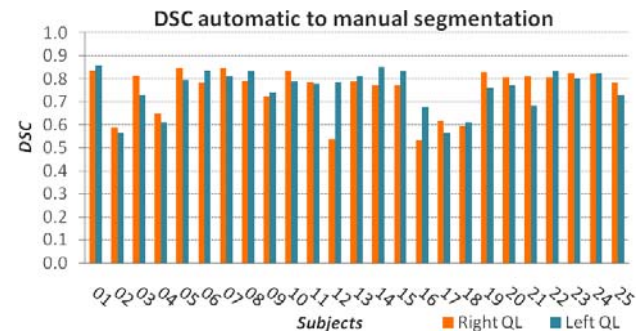


Figure.7. Dice Similarity Coefficients (DSC) of the automatic to manual segmentation for right and left QL.

Furthermore, automated segmentation of the QL was hampered by the proximity of other structures (e.g., kidneys) with similar signal intensity to the muscle which provided minimal contrast between the tissues.

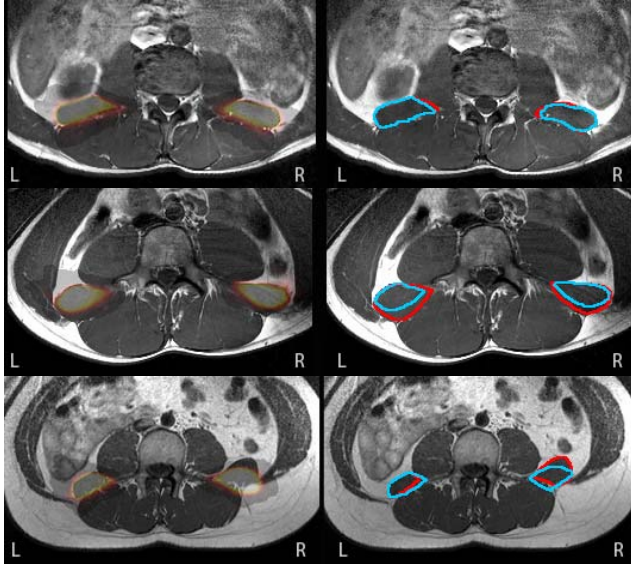


Figure 8. Upper pair of axial slices – subject with high DSC values (DSC: right QL 0.84, left QL 0.86). Middle pair - subject with left-right QL asymmetry 20% (DSC: right QL 0.56, left QL 0.61). Lower pair show subject with bulge on the left QL (DSC: right QL 0.8, left QL 0.62). Left images displays overlaid probabilistic map. Right images show differences between manual (red contour) and automatic (blue contour) segmentation.

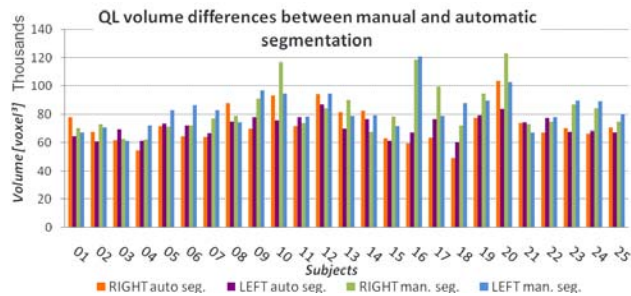


Figure 9. The QL volumes obtained from automatic and manual segmentation.

### 3.2 Quantitative Analysis

We performed the volumetric quantitative analysis of manually and automatically generated segmentations. Figure 9 illustrates how the volumetric results are particularly sensitive to the quality of automatic segmentation. With further optimization of the algorithm and generation of atlas from wider population the further improvement is expected.

### 3.3 Reproducibility of Quantitative Analysis

In terms of preliminary validation of the reproducibility of the automatic segmentation of the QL we calculated the (DSC coefficient) measures of left-right asymmetry on one subject (case 23 and 24). As can be seen in Figure 7 there is less than 3% difference in DCS score which is encouraging.

## 4. CONCLUSIONS AND FUTURE WORK

We have developed a promising *automated* segmentation procedure for determining bilateral QL muscle volumes based around a dedicated probability atlas of this paraspinal muscle. In order to improve the robustness of the automated segmentation of the QL and other paraspinal muscles such as the psoas, multifidus and erector spinae, further optimization of this approach will likely involve the hierarchization and generation of probability atlases for all the trunk muscles. Potentially, the use of multiple probability atlases across the thoracolumbar musculature will allow better separation along intermuscular septa and provide more robust volumetric data for individual muscles. Similarly, the addition of more sophisticated tissue classification methods should further enhance the atlas-based segmentation of the anatomically complex paraspinal muscles from adjacent abdominal fat and viscera. In future work we will incorporate the above methods on a larger MR dataset and examine the performance of the atlas-based approach for segmenting individual muscles with varying topologies (anatomic variations), asymmetries and trophic responses.

The results from the present atlas-based automated segmentation of the QL are encouraging and, with further developments, this approach could have ready application for morphometric analyses in large biomechanical studies and prospective examinations of preferential hypertrophy (atrophy) of the thoracolumbar muscles in (un)trained and injury states.

- [1] J. A. Hides, D. L. Belavy, W. Stanton, S. J. Wilson, J. Rittweger, D. Felsenberg, and C. A. Richardson, "Magnetic resonance imaging assessment of trunk muscles during prolonged bed rest," *Spine*, vol. 32, pp. 1687-1692, 2007.
- [2] K. L. Barker, D. R. Shamley, and D. Jackson, "Changes in the cross-sectional area of multifidus and psoas in patients with unilateral back pain - The relationship to pain and disability," *Spine*, vol. 29, pp. E515-E519, 2004.
- [3] S. Ourselin, A. Roche, G. Subsol, X. Pennec, and N. Ayache, "Reconstructing a 3D structure from serial histological sections," *Image and Vision Computing*, vol. 19, pp. 25-31, 2001.
- [4] D. Rueckert, L. I. Sonoda, C. Hayes, D. L. G. Hill, M. O. Leach, and D. J. Hawkes, "Nonrigid registration using free-form deformations: Application to breast MR images," *Ieee Transactions on Medical Imaging*, vol. 18, pp. 712-721, 1999.
- [5] L. R. Dice, "Measures of the Amount of Ecologic Association between Species," *Ecology*, vol. 26, pp. 297-302, 1945.
- [6] O. Salvado, C. Hillenbrand, S. X. Zhang, and D. L. Wilson, "Method to correct intensity inhomogeneity in MR images for atherosclerosis characterization," *Ieee Transactions on Medical Imaging*, vol. 25, pp. 539-552, 2006.
- [7] O. Salvado, C. M. Hillenbrand, and D. L. Wilson, "Partial volume reduction by interpolation with reverse diffusion," *International Journal of Biomedical Imaging*, vol. 2006, pp. 13, 2006.
- [8] T. Rohlfing, R. Brandt, R. Menzel, and C. R. Maurer, "Evaluation of atlas selection strategies for atlas-based image segmentation with application to confocal microscopy images of bee brains," *Neuroimage*, vol. 21, pp. 1428-1442, 2004.